Multiple Charge Extractions with Bias-flip Interface Circuit for Piezoelectric Energy Harvesting

Li Teng[1], Junrui Liang[1], and Zhiyuan Chen[2]
[1]School of Information Science and Technology, ShanghaiTech University, Shanghai 201210, China
[2]School of Microelectronics, Fudan University, Shanghai 201210, China
{tengli, liangjr}@shanghaitech.edu.cn, zhiyuan.chen@hotmail.com

***Abstract*— In piezoelectric energy harvesting (PEH), synchronous electric charge extraction (SECE) has the benefit of load independence. To reduce the energy dissipation on parasitic resistance, multi-shot SECE (MCE) was implemented to split the charge extraction process. In this paper, a multiple charge extraction with bias-flip (MCEBF) interface circuit is proposed. It not only reduces the dissipation in charge extraction but also enlarges the extractable energy of piezoelectric structure by adding a bias-flip action. MCEBF can also generate positive and negative voltage rails via buck-boost topology to supply power for double-rail devices. The analytical and experimental comparison among SECE, MCE, and MCEBF under different controls are also provided. In experiments, MCEBF offers a 57.3% improvement over SECE and 24% over MCE, in terms of harvested power.**

I. Introduction

Extracting energy from ambient vibration via energy harvesting (PEH) has shown its capability in some distributed and fully self-powered devices. Battery-free IoT nodes have received a great demand, which beckons more efficient and robust PEH solutions. In PEH, the power conditioning circuit can significantly influence the energy harvesting capability. Many PEH interface circuits have been proposed and studied. In synchronized switch harvesting on inductor (SSHI) [1] technology, the piezoelectric element is shorted by an inductor at each piezoelectric voltage peak to carry out a voltage bias-flip action, which enlarges the extracted energy. In synchronous electric charge extraction (SECE) [2] technology, source and load are isolated, energy in the piezoelectric capacitor is transferred to the storage by an inductor at each peak of piezoelectric voltage. To further reduce the energy dissipation in switching actions, the multi-shot control was introduced. An integrated multi-step SSHI interface circuit was proposed in [3], which can reduce the energy dissipation compared with conventional SSHI. An on-chip multi-shot SECE (MCE) solution was proposed in [4]. It can increase harvested power by 25% compared with SECE.

This paper introduces a new interface circuit by combining multiple charge extraction and bias-flip actions (MCEBF). Based on the measurement results, MCEBF can harvest 57.3% more power compared with SECE, and 24% more compared with MCE.

II. SECE and MCE

Fig. 1(a) shows the typical topology of SECE [2]. The i_{eq}, C_p, and R_p are the equivalent current source, piezoelectric capacitor, and dielectric resistance, respectively. These three elements model the piezoelectric equivalent under resonance. Compared with the standard energy harvesting (SEH) interface circuit, SECE can enhance the harvested power from the same piezoelectric vibration structure. Furthermore, the harvested power of SECE is independent of the load conditions [2]. As a result, maximum power point tracking (MPPT) is not required in SECE for maximizing the harvested power.

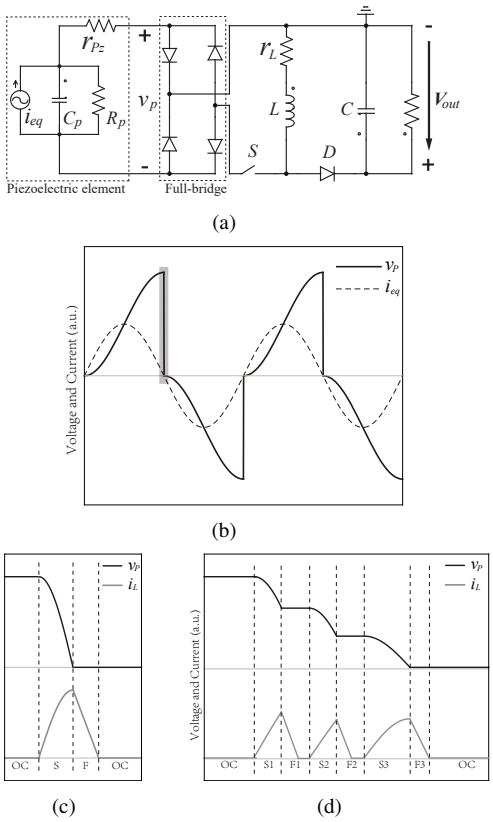

Fig. 1. Topology and waveforms of SECE and MCE interface circuit. (a) Typical topology of SECE interface circuit. (b) Piezoelectric voltage and equivalent current waveforms. (c) Enlarged view of a synchronized switch instant in SECE. (d) Enlarged view of a synchronized switch instant in 3CE

Fig. 1(b) and (c) show the working waveforms of SECE. In most of a period, the piezoelectric element is in open-circuit condition (specified as 'OC' phase in Fig. 1(c)). The switch and diode are off, the voltage across piezoelectric plate rises until it reaches $2V_{OC}$, where V_{OC} is the nominal

978-1-7281-3320-1/20/$31.00 ©2020 IEEE

Authorized licensed use limited to: ShanghaiTech University. Downloaded on November 07,2020 at 09:07:15 UTC from IEEE Xplore. Restrictions apply.

open-circuit voltage of the piezoelectric element. When the piezoelectric beam reaches its displacement extremes, the switch turns on. The circuit enters the switching phase ('S' phase). Piezoelectric capacitor C_p and the inductor L form an LC loop. A transient series oscillation happens through C_p and L. The 'S' phase lasts for $\pi\sqrt{LC_p}/2$. After the switching phase, the voltage across the piezoelectric plate drops to zero, while the inductor current reaches its maximum value. As the switch turns off, inductor current flows through the freewheeling diode. the circuit enters the free-wheeling phase ('F' phase), and charges the output capacitor C. After depletion of inductor current, the free-wheeling diode is reversely shut down. The circuit returns to open-circuit condition. In the switching and free-wheeling phases, there is some energy dissipation because of the equivalent series resistance (ESR) of piezoelectric element, on-state resistance of switch, and ESR of inductor L. As a result, the ESR of LC loop plays an important role towards the efficiency of SECE interface circuit. The energy dissipation can be expressed as follows [5]

$$E_{\mathrm{d,switch}} = 2(\gamma+1)C_pV_{\mathrm{oc}}^2, \tag{1}$$

where γ is the inversion factor mentioned in the SSHI topology [6], γ can be calculated as follows

$$\gamma = -e^{-\frac{\pi}{2Q}}, \tag{2}$$

where Q is the quality factor of the LC loop with an ESR.

To harvest more energy by using an LC circuit with a considerable ESR, the dissipation in ESR should be reduced. Thus, MCE was implemented [4], [7]. It can improve the harvesting capability by up to 25% according to the literature. MCE can be implemented on the same circuit configuration of SECE by varying the control method. It splits the switching and freewheeling phases into multiple steps. The voltage and current profiles look the same as those in SECE. Fig. 1(d) shows the enlarged view of the piezoelectric voltage and inductor current around a synchronized switch instant in 3CE (MCE with three extracting actions).With the alternate extraction and transfer phases, piezoelectric voltage drops in a stair shape (see 'S1' and 'S2' in Fig. 1(d)). In the last step, the switch turns on for the duration of $\pi\sqrt{LC_p}/2$. All residual energy is extracted by the inductor (see 'S3' in Fig. 1(d)), and further transferred to the output node. In MCE, the peak inductor current is suppressed, which reduces energy dissipation on ESR. Since the total extractable energy is the same, by reducing the energy dissipation in extraction, MCE can achieve higher harvested power, compared with SECE.

III. MCEBF

To further enhance the harvested power of PEH, besides reducing resistive dissipation, we should also increase the extracted energy. It can be achieved by adding a bias-flip action after the multiple charge extractions. The proposed MCEBF interface circuit is shown in Fig. 2. MCEBF is based on the buck-boost topology, which can isolate the piezoelectric source from the load. r_{Pz} and r_L are the ESRs

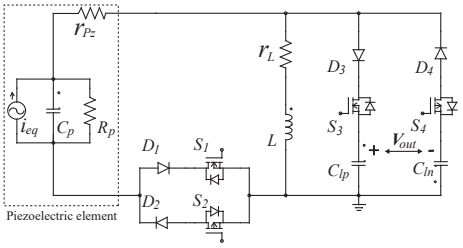

Fig. 2. Simplified schematic of MCEBF circuit

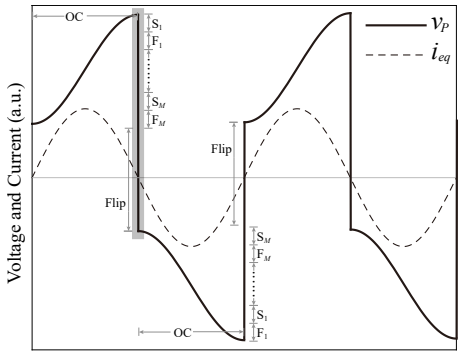

Fig. 3. Operating waveform of MCEBF circuit

of the piezoelectric plate and inductor. D_1 to D_4 and S_1 to S_4 are diodes and MOSFETs working as switches. C_{lp} and C_{ln} are the positive and negative load capacitors, respectively. They provide positive and negative voltage rails. In MCEBF, the inductor L has two functions. The first is to extract energy from the piezoelectric capacitor as SECE and MCE do. The second is to flip the residual charge after several rounds of extraction. Which is similar to that in SSHI. The operating waveforms of MCEBF are shown in Fig. 3. In each zero-crossing point of i_{eq} (see each edge of v_p in Fig. 3), there are M rounds of switching and freewheeling phases. For example, in the falling edge of voltage, assuming diodes are ideal and neglecting the energy dissipation in freewheeling phases, the operating principle can be analyzed as follows:

- **Open-circuit phase (OC)**: In the open-circuit phase, whose conducting branch and waveforms are shown in Fig. 4(a) and (b), all switches turn off. The piezoelectric element is in open-circuit condition. Equivalent current in piezoelectric element charges its internal capacitor C_p, until v_p rise for $2V_{OC}$.
- **Switching phases (S1, S2 ... SM)**: In the switching phases, as shown in Fig. 4(c) and (d), the piezoelectric capacitor is shunted by inductor L via MOSFET S_2 and diode D_2. As a result, the current through the inductor L will rise according to the duration of series RLC response. The duration of each switching phase t_s is set to a constant, and $t_s \ll \pi\sqrt{LC_p}/2$. Thus, the peak current of the inductor in the m^{th} switching phase can be formulated as follows

$$I_m = t_s\frac{V_{p,\,m-1}}{L}, \tag{3}$$

Authorized licensed use limited to: ShanghaiTech University. Downloaded on November 07,2020 at 09:07:15 UTC from IEEE Xplore. Restrictions apply.

where $V_{p,\,m-1}$ is the voltage across C_p after the $(m-1)^{th}$ round of switching and freewheeling phases. and $V_{p,\,m-1}$ can be formulated as follows

$$V_{p,\,m} = \left(1 - \frac{t_s^2}{2LC}\right) V_{p,\,m-1}. \tag{4}$$

Denoting the initial voltage as $V_{p,\,0}$, the expression of $V_{p,\,m}$ and I_m can be derived as follows

$$V_{p,\,m} = V_{p,\,0}\left(1 - \frac{t_s^2}{2LC}\right)^m, \tag{5}$$

$$I_m = \frac{V_{p,\,0}}{L}\left(1 - \frac{t_s^2}{2LC}\right)^{m-1}. \tag{6}$$

- **Freewheeling phases (F1, F2 ... FM)**: In the freewheeling phases, as shown in Fig. 4(e) and (f), switch S_2 turns off, and switch S_4 turns on. The energy stored in the inductor flows to the storage capacitor C_{ln}, which generates a more negative output voltage. The capacitance of the storage capacitor is designed to be much larger than that of C_p. The slope of the inductor current drop can be regarded as a constant value. When inductor current drops to zero, diode D_4 is reversely shut down. The freewheeling process ends.
- **Bias-flipping phase (Flip)**: The bias-flip phase is shown in Fig. 4(g) and (h). After M rounds of switching and freewheeling phases, the residual charge on C_p is flipped by the inductor. The end voltage $V_{p,\,M+1}$ of the flipping action can be expressed as follows

$$V_{p,\,M+1} = \gamma V_{p,\,M}. \tag{7}$$

The flipping phase is a little longer than $\pi\sqrt{LC_p}$ to ensure that the bias-flip action is complete. When the inductor current drops to zero, the branch is cut off by D_2.

After the falling edge bias-flip, the circuit starts another half cycle, the operating principle is the same, while the inductor current is negative and generates a positive output voltage. At steady state, $V_{p,\,0}$ can be expressed as follows

$$V_{p,\,0} = -V_{p,\,M+1} + 2V_{oc}, \tag{8}$$

by solving equations (5), (7) and (8), the initial voltage of each cycle $V_{p,\,0}$ can be obtained as follows

$$V_{p,\,0} = \frac{2V_{OC}}{\gamma\left(1 - \frac{t_s^2}{2LC}\right)^M + 1}. \tag{9}$$

The net harvested energy can be calculated as the difference between extracted energy from the piezoelectric element and dissipated energy in the ESR. The extracted energy in the m^{th} switching phase can be formulated in series:

$$\Delta E_m = \frac{1}{2}C_P\left(V_{p,\,m}^2 - V_{p,\,m-1}^2\right). \tag{10}$$

The energy dissipation in each phase is

$$E_{d,\,m} = \frac{1}{3}I_m^2 t_s\left(r_{\mathrm{L}} + r_{\mathrm{Pz}}\right). \tag{11}$$

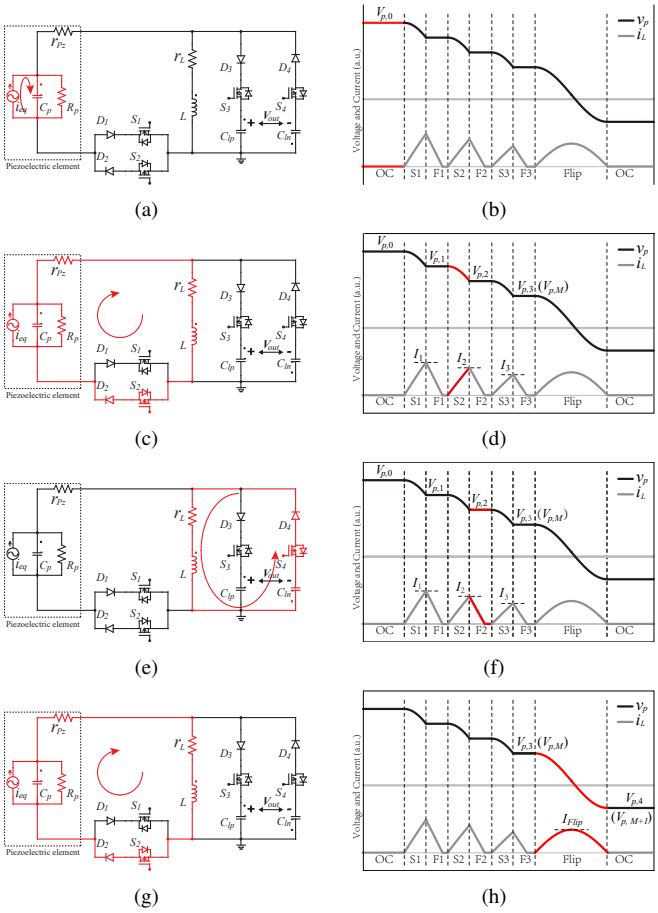

Fig. 4. Operating phases in the falling edge. (a)(c)(e)(g) Conduction branches. (b)(d)(f)(h) Waveforms of the piezoelectric voltage and inductor current. (a)(b) Open-circuit phase. (c)(d) One of the Switching phases. (e)(f) One of the Freewheeling phases. (g)(h) Bias-flipping phase.

TABLE I
CIRCUIT SPECIFICATIONS

C_p	r_{Pz}	r_L	L	γ	f
35 nF	500 Ω	200 Ω	200 mH	-0.63	20 Hz
V_{OC}	C_{ln}	C_{lp}	NMOS	PMOS	Diode
10 V	10 μF	10 μF	ZVN4424	ZVP4424	1N4002

thus, total harvested power can be expressed as the sum of the series:

$$P_h = 2f\sum_{m=1}^{M}\left(\Delta E_m - E_{d,\,m}\right), \tag{12}$$

where f is the operating frequency of the piezoelectric structure. Taking the number of shots M and the duration of each switching phase t_s as variables. Larger M gives higher harvested power. For t_s, the harvested power varies with different t_s. The harvested power of MCEBF as a function of t_s and M are plotted in Fig. 5, based on numerical calculation. The harvested power of MCE and SECE are also shown in Fig. 5. The circuit parameters are given in Table I.

In Fig. 5, the three surfaces stand for the power harvested via MCEBF, MCE, and SECE with the same circuit configuration.

Authorized licensed use limited to: ShanghaiTech University. Downloaded on November 07,2020 at 09:07:15 UTC from IEEE Xplore. Restrictions apply.

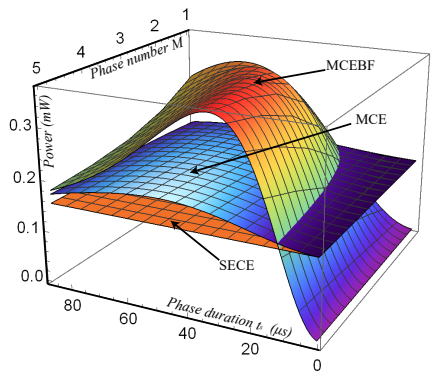

Fig. 5. Comparison of harvested power in MCEBF, MCE, and SECE.

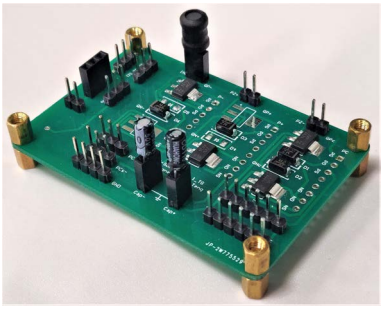

Fig. 6. PCB Prototype

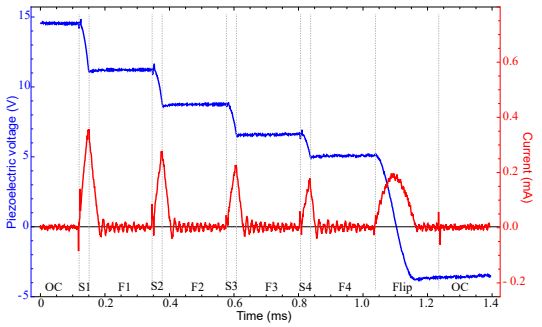

Fig. 7. Experimental piezoelectric voltage and inductor current waveform at a downstairs synchronized instant.

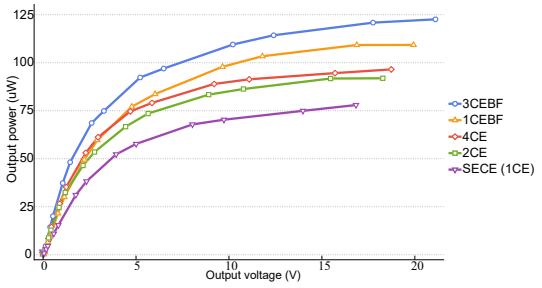

Fig. 8. Harvested power comparison among MCEBF, MCE, and SECE.

The harvested power varies under different t_s. Nevertheless, an optimal t_s value can be calculated based on the provided circuit parameters. The harvested power of MCE is always higher than SECE. While MCEBF outperforms MCE and SECE around the optimal point of t_s.

IV. Experiment

The printed circuit board (PCB) of MCEBF is shown in Fig. 6. Component parameters are listed in Table I. The switch signals are generated externally by a micro-controller.

The operating waveforms of 4CEBF (four rounds of charge extractions with bias-flip) are shown in Fig. 7. In experiment, there are four switching, four freewheeling phases, and one bias-flip phase in a half cycle. Fig. 7 shows the instant of falling edge, the same condition as that of Fig. 4. In 4CEBF, the energy is extracted gradually from the piezoelectric element by the inductor in four steps. During the harvesting process, the piezoelectric voltage drops in a stair shape. The inductor current peak gets lower compared with the former one. After 4 steps of energy extraction, the residual charge is flipped to pre-bias the voltage for the reverse-charging in the next half cycle.

SECE and MCE can also be implemented by changing the control on this circuit. By sweeping the load resistance connected between positive and negative output nodes, the harvested power as a function of the output voltage is plotted in Fig. 8.

Compared with conventional SECE, 2CE can harvest 17% more power. The more shots in energy extraction, the less energy dissipation. On the other hand, 1CEBF (one charge extraction with bias-flip) can increase the harvested power by 40.1%. While 3CEBF (three rounds of charge extractions with bias-flip) can harvest 57.3% more power compared with SECE. The output power approaches to constants when the output voltage is above 10V (see Fig. 8), which means that the harvested power of MCEBF is also insensitive to the load condition. Based on the measurement results, MCEBF can significantly improve the harvesting capability compared with SECE and MCE. The merit of load independence in SECE is inherited in MCEBF. That means the optimal output power can be maintained in a wide range of load conditions, MPPT is not necessary for MCEBF.

V. Conclusion

This paper introduced a multiple charge extraction with bias-flip (MCEBF) interface circuit for piezoelectric energy harvesting (PEH). It extracts electric charges on the piezoelectric element with multiple steps and flips the residual charge with bias-flip action. MCEBF not only reduces the dissipation in the equivalent series resistance (ESR) but also enlarges the extracted energy. The effectiveness of MCEBF is studied theoretically. In experiment, an improvement of 57.3% more harvested power is obtained, compared with the synchronous electric charging extraction (SECE).

Acknowledgment

The work described in this paper was supported by the grants from National Natural Science Foundation of China (Project No. 61401277) and ShanghaiTech University (Project No. F-0203-13-003).

Authorized licensed use limited to: ShanghaiTech University. Downloaded on November 07,2020 at 09:07:15 UTC from IEEE Xplore. Restrictions apply.

REFERENCES

[1] D. Guyomar, A. Badel, E. Lefeuvre, and C. Richard, "Toward energy harvesting using active materials and conversion improvement by non-linear processing," *IEEE transactions on ultrasonics, ferroelectrics, and frequency control*, vol. 52, no. 4, pp. 584–595, 2005.

[2] E. Lefeuvre, A. Badel, C. Richard, and D. Guyomar, "Piezoelectric energy harvesting device optimization by synchronous electric charge extraction," *Journal of Intelligent Material Systems and Structures*, vol. 16, no. 10, pp. 865–876, 2005.

[3] S. Javvaji, V. Singhal, V. Menezes, R. Chauhan, and S. Pavan, "Analysis and design of a multi-step bias-flip rectifier for piezoelectric energy harvesting," *IEEE Journal of Solid-State Circuits*, vol. 54, no. 9, pp. 2590–2600, 2019.

[4] P. Gasnier, J. Willemin, S. Boisseau, G. Despesse, C. Condemine, G. Gouvernet, and J.-J. Chaillout, "An autonomous piezoelectric energy harvesting ic based on a synchronous multi-shot technique," *IEEE Journal of Solid-State Circuits*, vol. 49, no. 7, pp. 1561–1570, 2014.

[5] C. Chen, B. Zhao, and J. Liang, "Revisit of synchronized electric charge extraction (sece) in piezoelectric energy harvesting by using impedance modeling," *Smart Materials and Structures*, vol. 28, no. 10, p. 105053, 2019.

[6] J. Liang and W. Liao, "Piezoelectric energy harvesting and dissipation on structural damping," *Journal of Intelligent Material Systems and Structures*, vol. 20, no. 5, pp. 515–527, 2009.

[7] S. Chamanian, H. Uluşan, A. Koyuncuoğlu, A. Muhtaroğlu, and H. Külah, "An adaptable interface circuit with multistage energy extraction for low-power piezoelectric energy harvesting mems," *IEEE Transactions on Power Electronics*, vol. 34, no. 3, pp. 2739–2747, 2018.

Authorized licensed use limited to: ShanghaiTech University. Downloaded on November 07,2020 at 09:07:15 UTC from IEEE Xplore. Restrictions apply.